ASSESMENT OF COMPOSITE DELAMINATION SELF-HEALING VIA MICRO-ENCAPSULATION

T. Kevin O'Brien
U.S. Army Research Laboratory
Vehicle Technology Directorate
Durability, Damage Tolerance & Reliability Branch
NASA Langley Research Center
Hampton, VA

Scott R. White
Aerospace Engineering Department
University of Illinois
Urbana-Champaign, Illinois

To be published in Proceedings of
American Society for Composites
23rd Technical Conference
Memphis, Tennessee
Sept. 2008

ABSTRACT

Composite skin/stringer flange debond specimens manufactured from composite prepreg containing interleaf layers with a polymer based healing agent encapsulated in thin walled spheres were tested. As a crack develops and grows in the base polymer, the spheres fracture releasing the healing agent. The agent reacts with catalyst and polymerizes healing the crack. In addition, through-thickness reinforcement, in the form of pultruded carbon z-pins were included near the flange tips to improve the resistance to debonding. Specimens were manufactured with 14 plies in the skin and 10 plies in the stiffener flange. Three-point bend tests were performed to measure the skin/stiffener debonding strength and the recovered strength after healing. The first three tests performed indicated no healing following unloading and reloading. Micrographs showed that delaminations could migrate to the top of the interleaf layer due to the asymmetric loading, and hence, bypass most of the embedded capsules. For two subsequent tests, specimens were clamped in reverse bending before reloading. In one case, healing was observed as evidenced by healing agent that leaked to the specimen edge forming a visible "scar". The residual strength measured upon reloading was 96% of the original strength indicating healing had occurred. Hence, self-healing is possible in fiber reinforced composite material under controlled conditions, i.e., given enough time and contact with pressure on the crack surfaces. The micro-encapsulation technique may prove more robust when capsule sizes can be produced that are small enough

to be embedded in the matrix resin without the need for using an interleaf layer. However, in either configuration, the amount of healing that can occur may be limited to the volume of healing agent available relative to the crack volume that must be filled.

INTRODUCTION

Recently, the promise of self-healing materials for enhanced autonomous durability has been introduced using the micro-encapsulation technique [1]. In this technique, a polymer based healing agent is encapsulated in thin walled spheres and embedded into a base polymer along with a catalyst phase (fig.1).

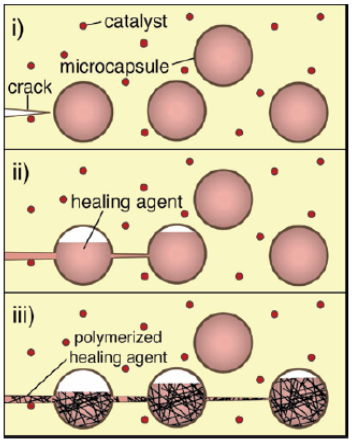

Fig.1 Micro-encapsulation technique for self-healing

As a crack develops and grows in the base polymer, the spheres fracture, releasing the healing agent. The agent reacts with catalyst polymerizing and healing the crack. Using a height-tapered Double Cantilever Beam (DCB) fracture specimen, White, et.al. demonstrated recovery of 90% of the virgin fracture toughness of the base polymer [1]. This technique was recently applied to the resin matrix of a fiber reinforced composite material [2]. An interleaf prepreg material was manufactured where the interleaf layer contained the micro-encapsulated healing agent. This prepreg was used to manufacture composite coupon specimens, consisting of a skin and a flange tip, designed to study skin/stiffener debonding [3,4]. In addition, through-thickness reinforcement, in the form of pultruded carbon z-pins were included near the flange tips to improve the resistance to debonding [5,6]. By combining these two technologies, it was hoped to obtain a synergy between the damage tolerance provided by the z-pins and the durability provided by the self-healing matrix.

PREPREG MATERIAL

Two forms of self-healing prepreg material were considered, direct embedding and interlayers (fig. 2).

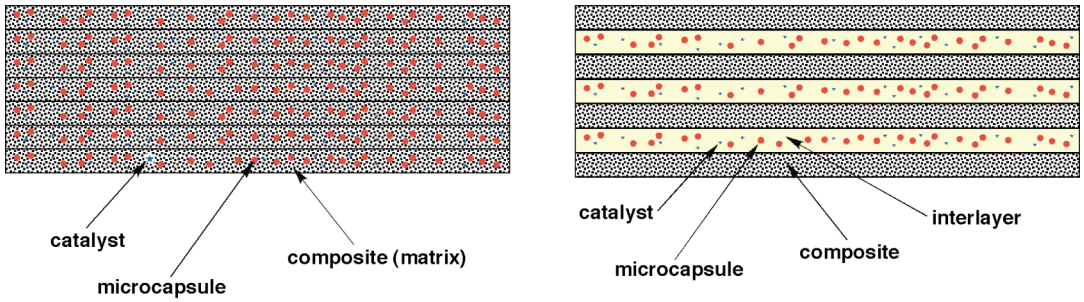

(a) Direct embedding (b) Interleaf

Fig.2 Two approaches for self-healing prepreg

In the direct embedding approach, a homogeneous distribution of the microcapsules and catalyst is desired in the matrix phase during wet winding. A filament winding technique was developed to fabricate self-healing fiber-reinforced polymeric matrix prepreg material for material characterization and concept validation [2]. The base matrix resin consisted of Epon 862® with an Epicure 3274® curing agent. This material cures at room temperature, achieving a tack free cure overnight and a full cure in seven days. Polymer shell microcapsules, 10-100 μm in diameter, were produced and filled with a dicyclopentadiene (DCPD) healing agent. A wet-winding process was used to produce the composite prepreg, where IM7-GP 12K carbon fiber bundles passed through a resin bath before being wound onto the mandrel. The microcapsules and catalyst were dispersed in the resin bath for incorporation in the prepreg matrix. Continuous prepreg sheets were produced and then cut from the mandrel. During initial trials, nearly half the capsules were either not picked up by the fibers or did not survive the filament winding process. In the interlayer approach, microcapsules and catalyst were dispersed in the base resin bath and deposited onto a carrier fabric on the top of each composite layer containing the base resin only with no healing agent. This composite plus interlayer ply was then wound on the mandrel. Continuous prepreg sheets were produced and then cut from the mandrel. This procedure allowed the majority of the self-healing capsules to survive the filament winding process. Hence, the resin interlayer was deemed to be a more viable approach at that time for incorporating microcapsules into composite prepreg.

PANEL MANUFACTURE AND SPECIMEN PREPARATION

Two types of prepreg materials were produced and shipped to Boeing, Philadelphia, to manufacture the composite panels. One prepreg type included the base resin only (no self-healing interlayer), whereas the other prepreg type included the base resin plus the self-

healing interlayer. Seven panels were layed up and cured on a vacuum debulk table at 95°F for 48 hours using a 15 psi vacuum bag pressure. Two panels were manufactured using the base resin matrix only. Two panels were manufactured with self-healing material only in six plies, three on either side of flange-to-skin bond line. Three panels were manufactured with all self-healing plies where each ply in the skin and stiffener flange contained an interleaf layer with the microencapsulated healing agent. One panel of each type had no z-pin reinforcement. The others had 0.5% or 1.0% density z-pins on either side of the flange tip. Z-pins were inserted using an ultrasonic hammer after panel lay-up but prior to curing under pressure. Twelve-inch-square panels were manufactured with 14 plies in the skin, with a $[45/90/-45/0/45/0/-45]_s$ orientation, and 10 plies with a $[45/90/-45/0/90]_s$ orientation in the two stiffener flange strips. Table I summarizes the panels made.

Table I Skin/stringer flange panels produced

Panel #	Self-healing interlayer	Z-pin density
1	none	none
2	none	1.0%
3	6 plies near bondline	none
4	6 plies near bondline	1.0%
5	All plies	0.5%
6	All plies	none
7	All plies	1.0%

The first two panels made with the base resin had significant regions of resin starvation (fig.3). This was believed to be a result of partial cure and/or moisture infusion due to a loss of refrigeration in transit because the prepreg was shipped using gel-packs instead of dry ice. The two panels made with self-healing material only in six plies, three on each side of flange-to-skin bond line, had smooth surfaces on the top of the skin where the interlayer was exposed, but were also resin starved on the bottom of the skin and top of the flange strips that had only the base resin (fig.4).

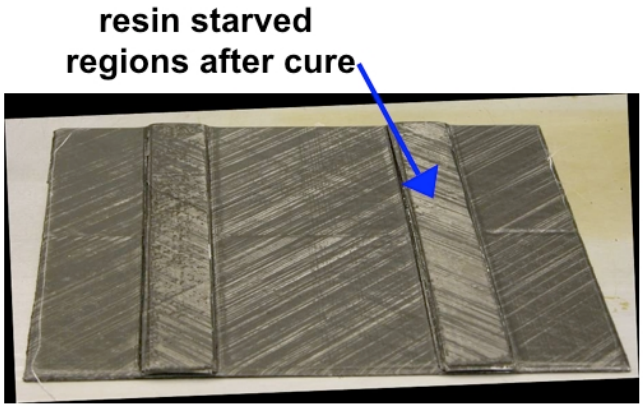

Fig.3 Skin/stringer flange panel with base resin only

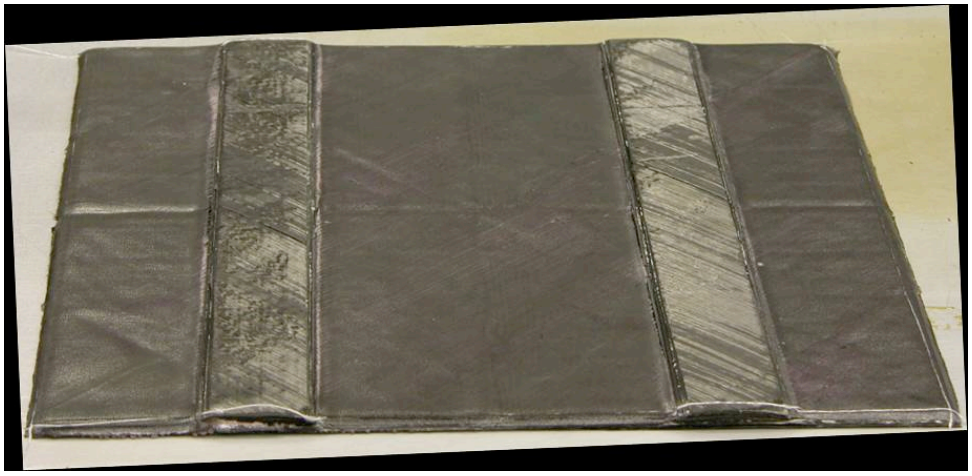

Fig.4 Skin/stringer flange panel with self-healing material only in three plies on either side of flange-to-skin bond line

The three panels made with self-healing material throughout, i.e., each ply in the skin and stiffener flange contained an interleaf layer with the microencapsulated healing agent, had smooth surfaces. For the two panels with z-pins, some compaction was evident in the regions near the flange tip where the z-pins were applied (fig. 5).

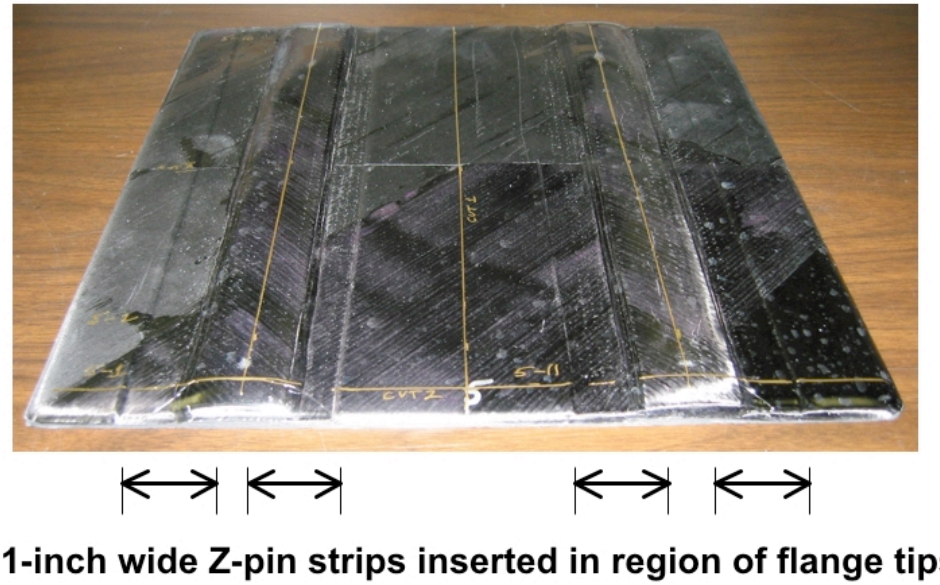

Fig.5 Skin/stringer flange panel with 0.5% density z-pins and self-healing material throughout

Figure 6 compares the total panel thicknesses (skin plus flange) calculated assuming the nominal prepreg ply thicknesses and the average panel thicknesses measured at the mid-point of the flange for the seven panels produced. Each interlayer was approximately 0.005 inches thick, which is roughly one-half the nominal thickness of the base resin ply (0.01 in). All seven panels had the same amount of fiber reinforcement. Hence, addition of the self-healing interlayers increased the panel thickness, and hence, reduced the effective fiber volume fraction. In some cases, the z-pins resisted the vacuum bag pressure, and hence, also increased panel thickness and reduced the fiber volume fraction.

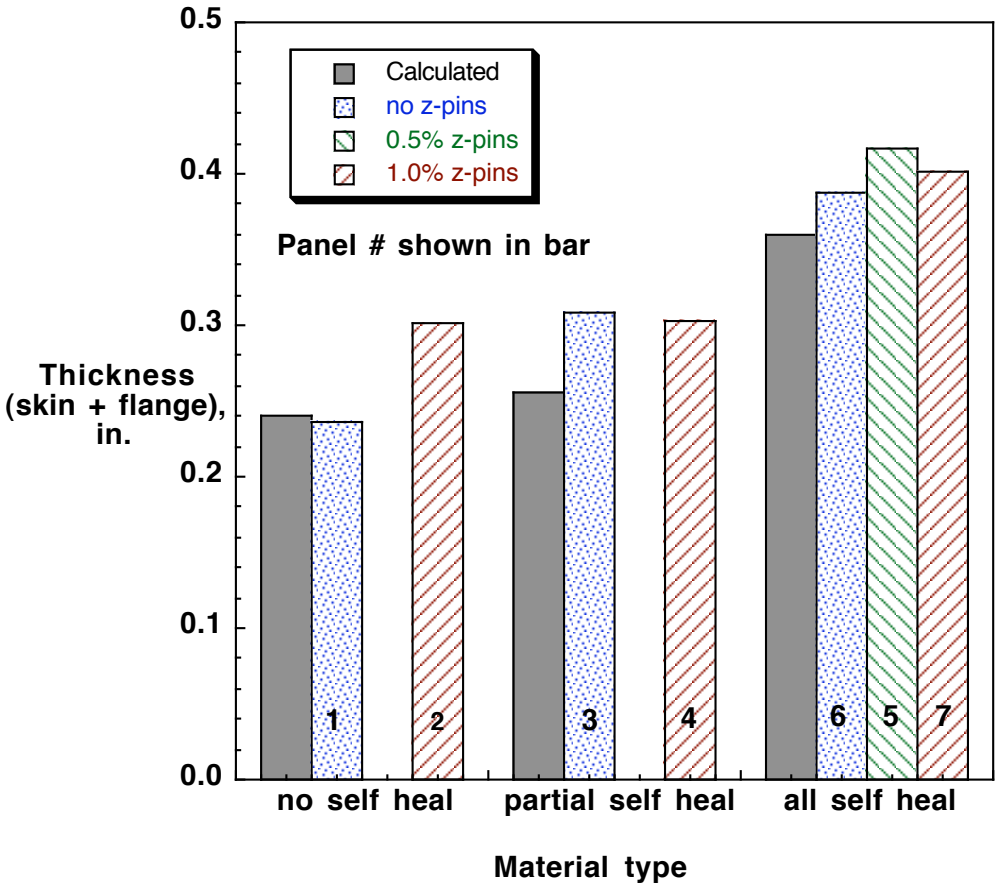

Fig.6 Comparison of average panel thicknesses (skin + flange)

Panels were shipped to NASA Langley for cutting and testing. Twenty coupons, six-inches long by one-inch-wide, representing a stiffener flange bonded to a skin (fig.7) were cut from each panel for three-point-bend testing.

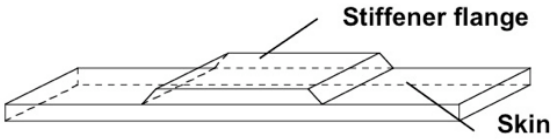

Fig. 7 Skin/stiffener flange debond specimen configuration

Figure 8 shows a micrograph of the edge of a specimen with self-healing material only in three plies on either side of the flange-to-skin bond line. Several ply interfaces are missing an interleaf layer, while others have double interleaf layers. This was a result of a prepreg orientation error during lay up of the panel. Unfortunately, both of the panels with self-healing material only in three plies on either side of the flange-to-skin bond line contained layup errors, and hence, were not tested.

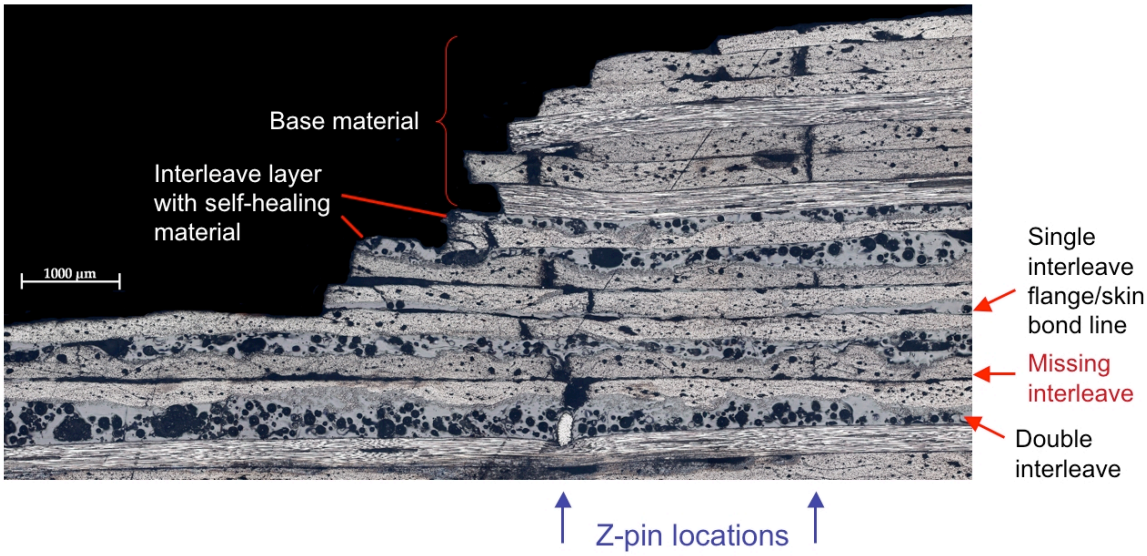

Fig. 8 Micrograph of edge of specimen with self-healing material only in three plies on either side of flange-to-skin bond line

For two of the three panels with self-healing material throughout, several ply interfaces were missing an interleaf layer, while others had double interleaf layers. Unfortunately, only specimens from panel #5 were free of these layup errors, and hence, these were the only ones tested. Figure 9 shows a micrograph of the edge of a specimen with self-healing material throughout from panel #5.

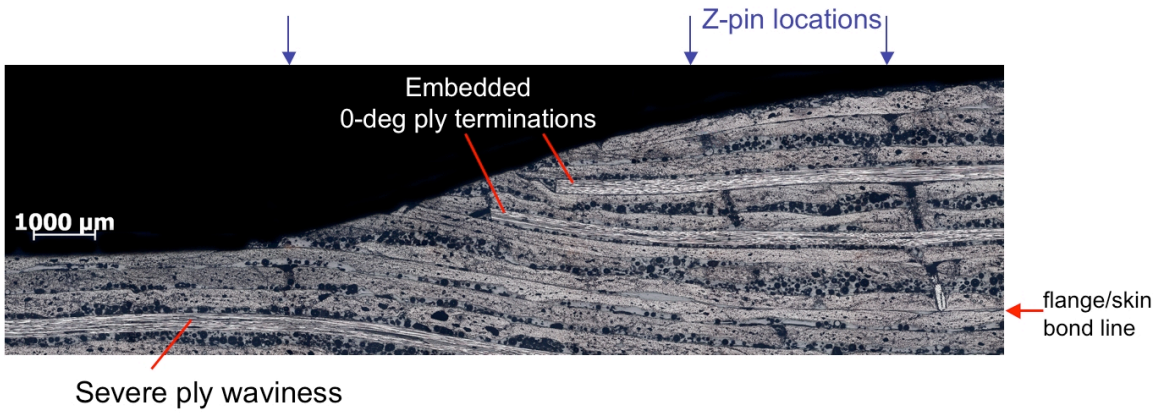

Fig.9 Micrograph of the edge of a specimen with self-healing material throughout

This panel had 0.5% density z-pins embedded near the flange tip. Unfortunately, the low fiber volume fraction allowed resin movement under pressure during cure resulting in (1) significant fiber waviness, (2) embedding of 0-degree ply terminations in the flange, and (3) shifting of z-fiber reinforcement from normal orientation (fig.9).

TEST PROCEDURE

Three-point-bend tests, with a five-inch span between the rollers, were performed to measure the skin/stiffener debonding strength and the recovered strength after healing (fig.10).

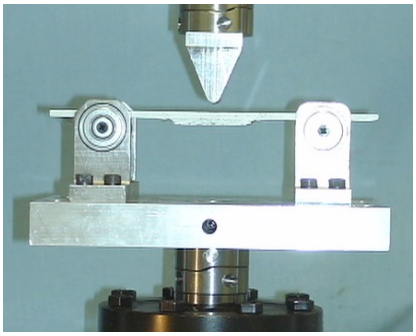

Fig.10 Three-point bend test set-up

All tests were performed using the set-up shown in figure 10 except the first test where the center of the specimen was loaded with a roller (similar to the two end supports shown in figure 10). All subsequent tests were performed using the central solid load nose shown in figure 10 to allow a better view of damage growth from both flanges during the test. Specimen edges were painted white, using a thin coat of spray paint, to easily detect the

onset and growth of damage. Tests were performed in a 5-kip hydraulic test stand at a stroke rate of 0.5 in/min.

As shown in table II, the first three specimens were loaded until damage formed at the flange tip(s), then reloaded after a hold time of 24 hours. The last two specimens were loaded until damage formed at the flange tip(s), then subjected to reverse bending during the hold time of 24-48 hours to effectively clamp the fracture surfaces together under pressure before reloading (fig.11).

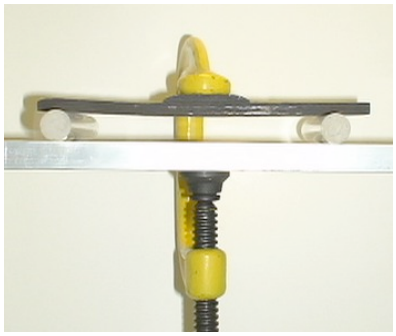

Fig.11 Reverse bending clamp-up

Table II Summary of test conditions

Specimen number	Hold time (hours)	Reverse bending clamp-up
5-06	24	no
5-20	24	no
5-17	24	no
5-10	48	yes
5-13	24	yes

TEST RESULTS

The first three tests (specimens number 5-06, 5-20, and 5-17) did not exhibit any evidence of self-healing. A detailed description of each test follows.

Figure 12 shows the load deflection plots for specimen 5-06. The specimen was inserted in the three-point bend fixture and loaded until damage developed. Inclusion of the interleaf in each ply resulted in relatively low fiber volume fractions, and hence, a viscoelastic response was obtained as evidenced by large hysteresis in the load-displacement plot (fig.12). Figure 13 shows the damage that developed at one flange tip on the edges. No damage developed at the other flange tip.

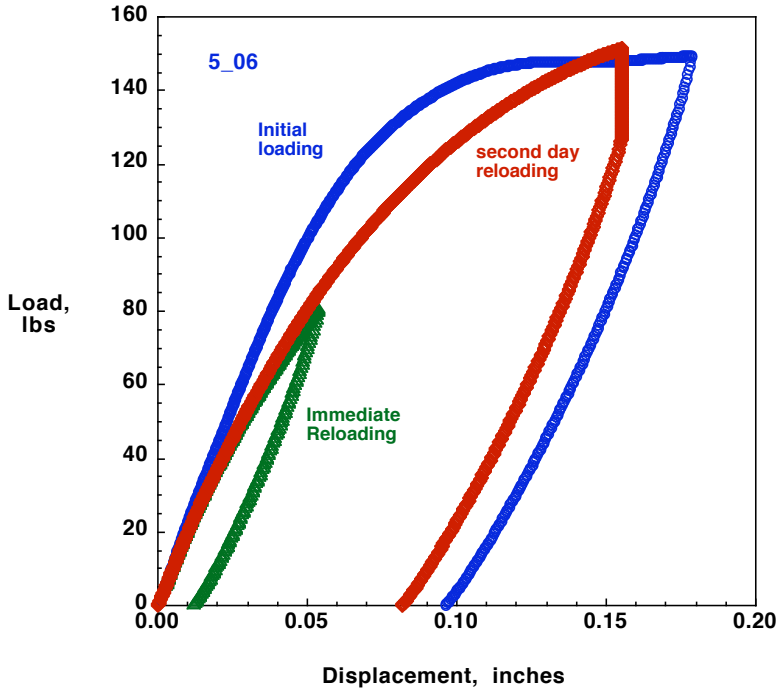

Fig.12 Load-displacement response for specimen 5-06

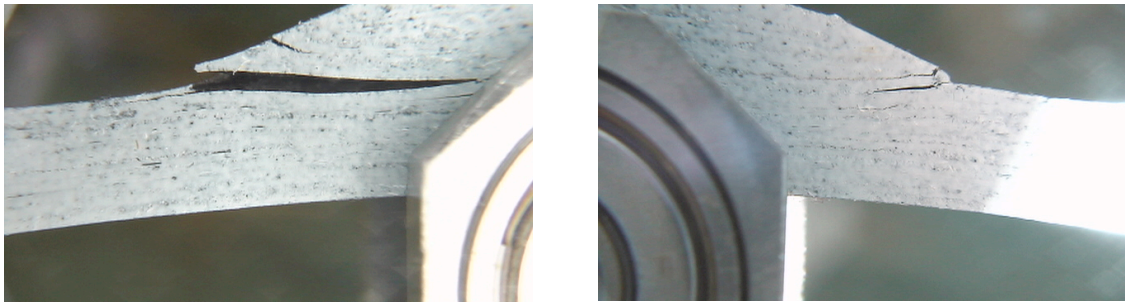

Fig. 13 Delamination at flange tip in specimen 5-06

After the specimen recovered to zero deflection, a second smaller load was applied immediately (fig.12). Some loss in stiffness was evident. The specimen was removed from the fixture for a 24-hour hold period. The specimen was re-inserted in the three-point bend fixture and reloaded until damage developed at a different location. The stiffness was nearly identical to the first immediate reloading (fig.12) indicating that no significant healing occurred following unloading and reloading. There was no visual evidence of healing on the specimen edges.

Figure 14 shows the initial load deflection plot for specimen 5-20. The specimen was inserted in the three-point bend fixture and loaded until damage developed. Figure 15 shows that the initial damage occurred at one flange tip with some evidence of z-pin pull-out. No damage developed at the other flange tip.

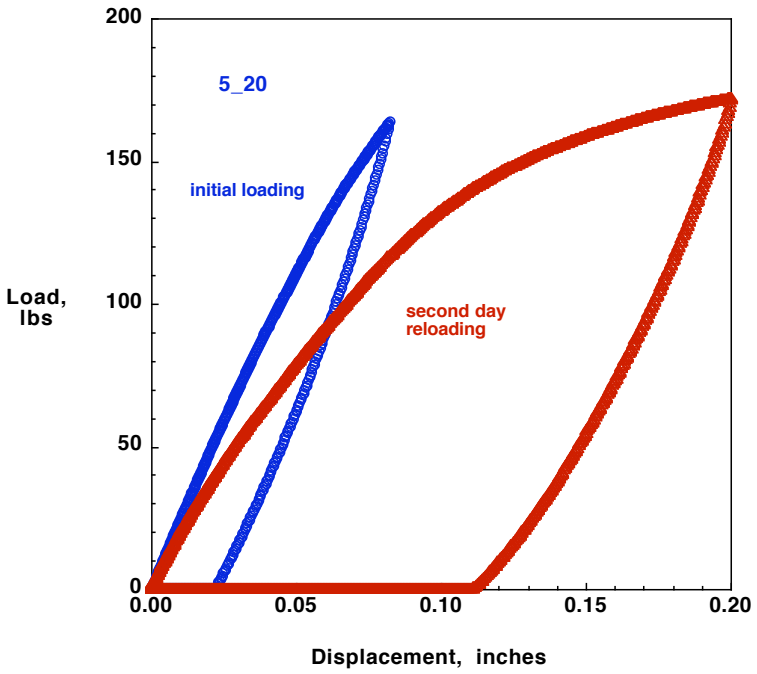

Fig.14 Load-displacement response for specimen 5-20

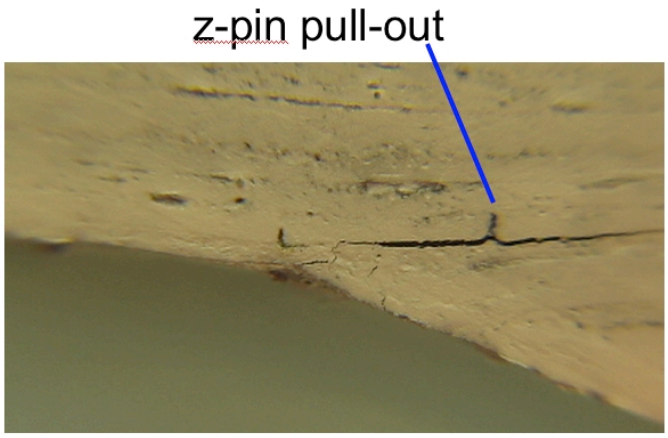

Fig. 15 Delamination at flange tip in specimen 5-20

After a 24-hour hold, the specimen was re-inserted in the three-point bend fixture and loaded to extend the original damage (fig.14). The stiffness was significantly less than the original stiffness, indicating that no significant healing occurred between unloading and reloading. There was no visual evidence of healing on the specimen edges.

Fig. 16 shows the initial load deflection plot for specimen 5-17. The specimen was inserted in the three-point bend fixture and loaded until significant damage had occurred at both flange tips. At the highest load applied, a secondary delamination formed in the skin (fig.17).

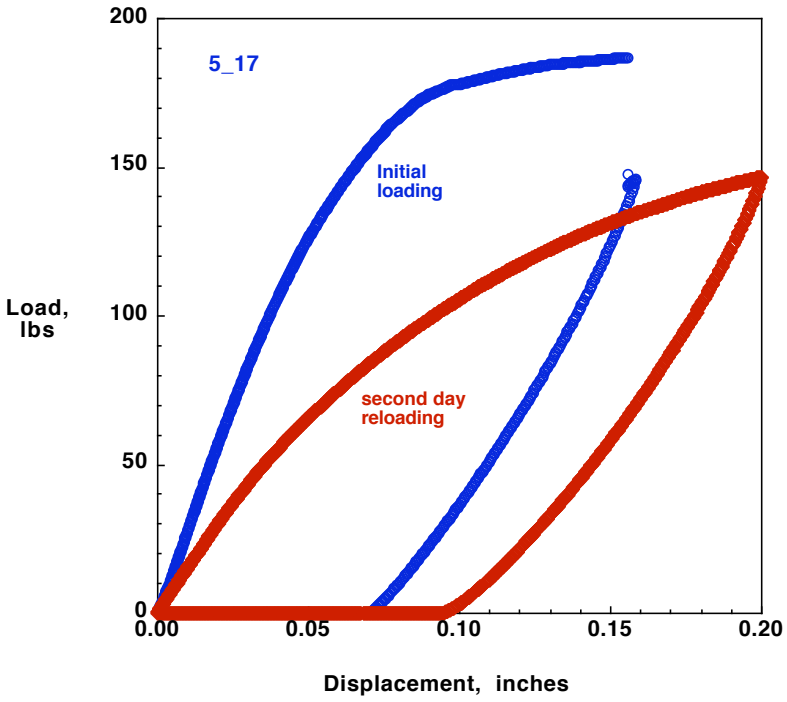

Fig.16 Load-displacement response for specimen 5-17

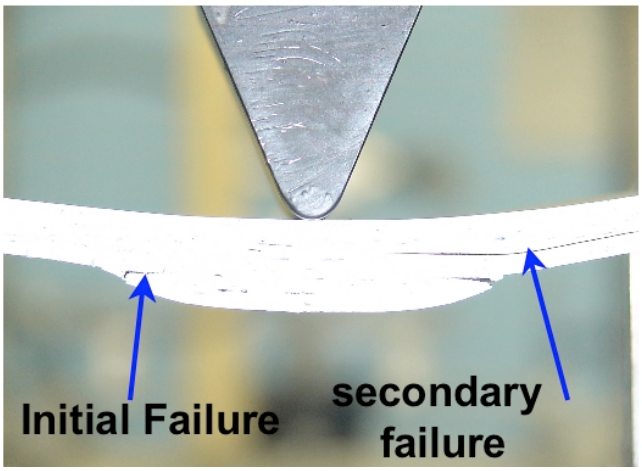

Fig. 17 Delamination at both flange tips and skin of specimen 5-17

After a 24-hour hold, the specimen was re-inserted in the three-point-bend fixture and loaded until it failed once again. This test indicated that no healing occurred between unloading and reloading. There was no visual evidence of healing on the specimen edges. The specimen was polished to remove the coating of white spray paint and to examine the damage in the optical microscope. Micrographs of the initial failure location showed that delaminations migrated to the top of the interleaf layer, and hence, bypassed most of the embedded capsules (fig.18). Micrographs indicated that the secondary delamination in the skin may have formed during the original loading due to the presence of three large voids in close proximity to each other (fig.19).

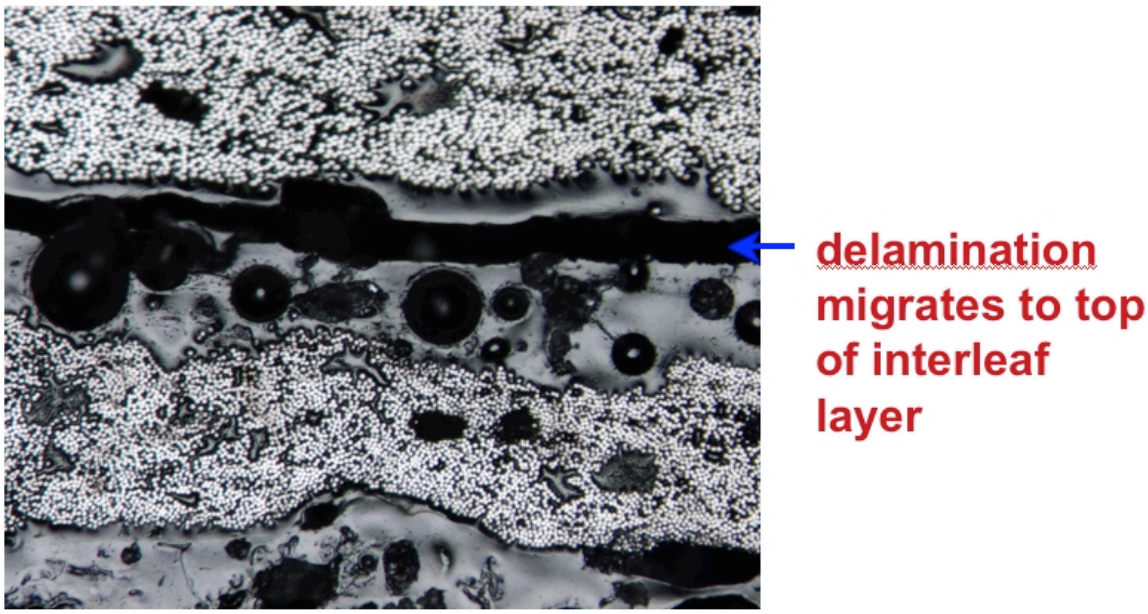

Fig.18 Micrograph showing delamination migration to top of interlayer

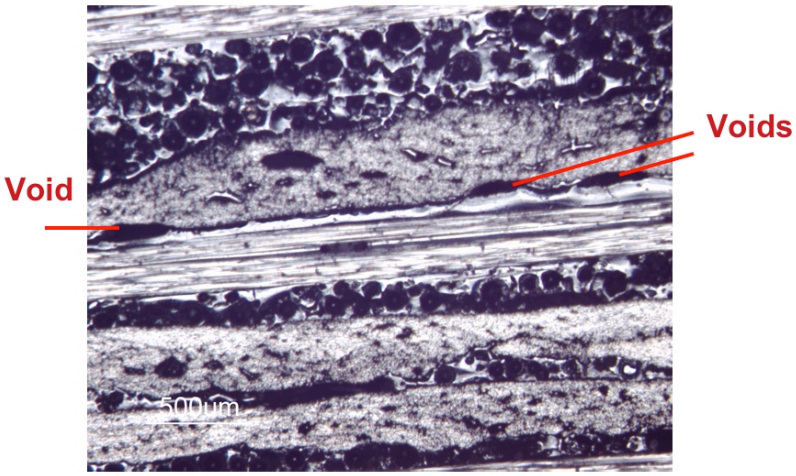

Fig.19 Micrograph showing secondary delamination in skin due to voids

The last two tests (specimens number 5-10, and 5-13) did exhibit some evidence that self-healing has occurred. A detailed description of each test follows.

Figure 20 shows the initial load deflection plot for specimen 5-10. The specimen was inserted in the three-point bend fixture and loaded until damage had occurred at both flange tips (fig.21).

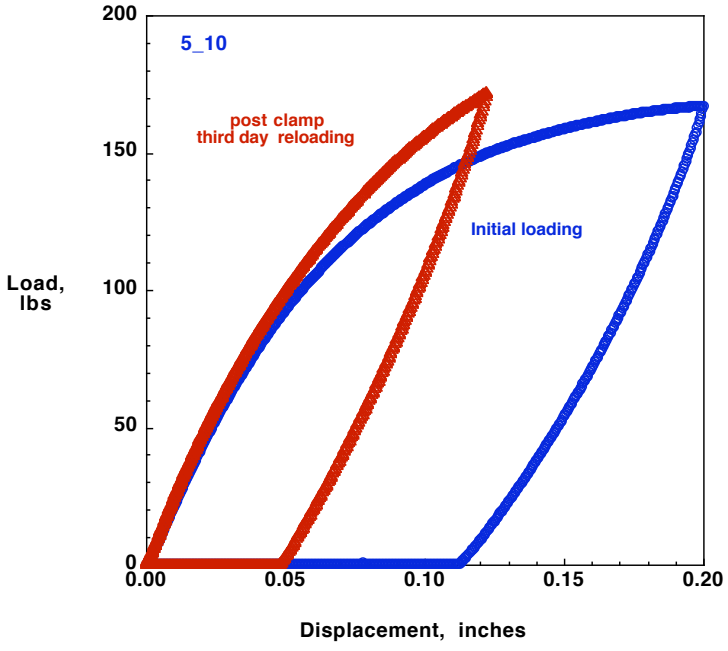

Fig.20 Load-displacement response for specimen 5-10

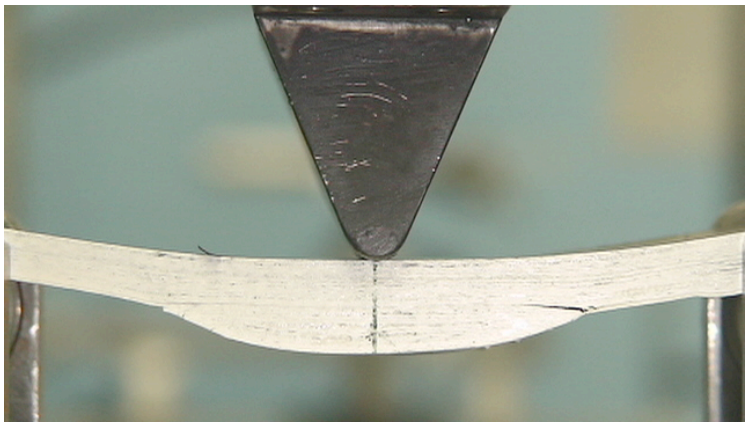

Fig. 21 Delamination at both flange tips of specimen 5-10

Upon removal from the three-point bend fixture, this specimen was clamped for 48 hours in reverse bending before re-loading (fig.11). Upon removal of the clamp, a residual curvature was evident. The original crack surfaces appeared to be closed, indicating that some healing may have occurred (fig.22). This reverse curvature resulted in a stiffer response upon reloading the specimen (fig.20). In addition, the specimen reached a slightly higher load than was obtained in the original loading before failure re-initiated.

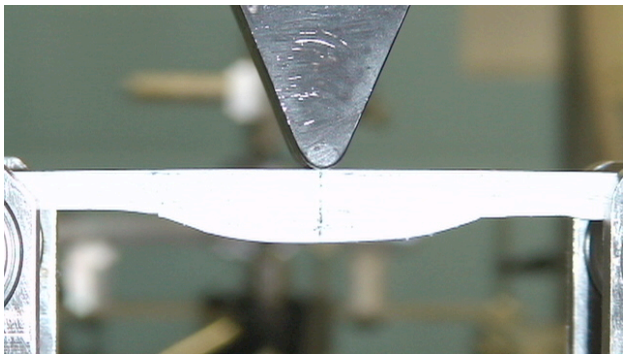

Fig.22 Residual curvature due to reverse bending clamp-up

Figure 23 shows the initial load deflection plot for specimen 5-13. The specimen was inserted in the three-point bend fixture and loaded until damage had occurred at one flange tip (fig.24).

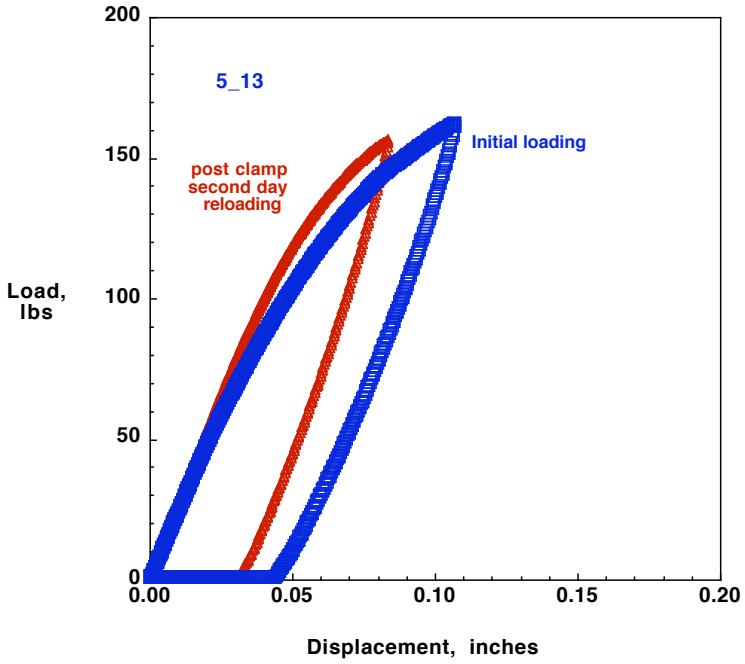

Fig.23 Load-displacement response for specimen 5-13

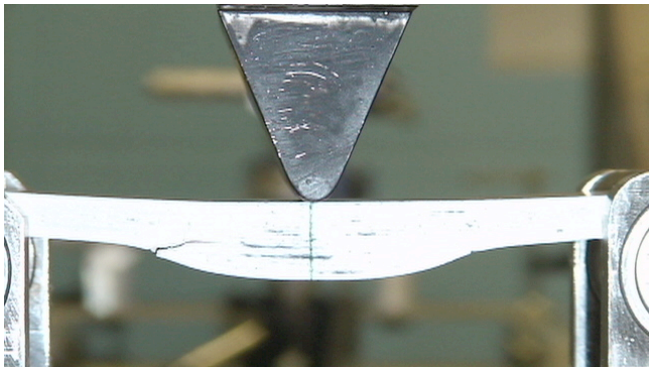

Fig. 24 Delamination at flange tip of specimen 5-13

Upon removal from the three-point bend fixture, this specimen was clamped in reverse bending before re-loading (fig.11). The specimen remained clamped for 24 hours. Upon removal of the clamp, a residual curvature was evident. The original crack surfaces appeared to be closed, indicating that some healing may have occurred. In addition, healing was observed as evidenced by healing agent that leaked to the specimen edge forming a visible "scar" (fig.25).

Fig.25 Visible post clamp-up "scar" indicating healing in specimen 5-13

The reverse curvature resulted in a stiffer response upon reloading the specimen (fig.23). Specimen 5-13 reached 96% of the original loading before failure re-initiated.

DISCUSSION

This current study evaluated the potential to achieve self-healing in fiber reinforced composites made with currently available, room temperature cured, polymer matrices using a single microencapsulated healing agent with the minimum capsule size available at the time. Although some self-healing was demonstrated, significant time at pressure was required to realize this goal. This was achieved by clamping the specimens in reverse bending during the 1-2 day hold time between the initial loading and reloading. Ultimately, new healing agents need to be developed that can (1) survive autoclave temperature and pressure cure cycles and (2) heal rapidly under load with minimal contact, in order to realize the potential for this technology. Furthermore, reducing the capsule size would enable incorporation of capsules within the base resin rather than adding an interleaf layer that (1) creates potential for lay-up errors that mitigate the benefit, (2) increases thickness and weight and reduces fiber volume fraction, and (3) allows crack migration to the interface where the capsules that are present may not fracture and release the healing agent. Since the development of the prepreg used in this study, further advances in capsule size reduction have been achieved [7]. However, as the capsule size decreases, the amount of healing agent is also reduced, limiting the ability to heal the crack volume. New techniques, such as the development of microvascular networks, are currently being developed to overcome some of these limitations [8].

CONCLUSIONS

This assessment demonstrated that self-healing is possible in fiber reinforced composite material under controlled conditions, i.e., given enough time and contact with pressure on the crack surfaces. The micro-encapsulation technique may prove more robust when capsule sizes can be produced that are small enough to be embedded in the matrix resin without the need for using an interleaf layer. However, in either configuration, the amount of healing that can occur may be limited to the volume of healing agent available relative to the crack volume that must be filled.

REFERENCES

1. White, S. R., Sottos, N. R., Geubelle, P. H., Moore, J. S., Kessler, M. R., Sriram, S.R., Brown, E.N., and Viswanathan, S. 2001. "Autonomic healing of polymer composites," *Nature* 409: pp.794-797.
2. Armagan, O., "Fiber-reinforced prepreg composites with self-healing matrices," MS Thesis, Department of Materials Science and Engineering, University of Illinois at Urbana-Champaign, September, 2006.
3. Minguet, P.J, and O'Brien, T.K., "Analysis of Test Methods for Characterizing Skin/Stringer Debonding Failures in Reinforced Composite Panels," *Composite Materials: Testing and Design, Twelfth Volume*, ASTM STP 1274, August, 1996, pp.105-124.
4. Krueger, R., Cvitkovich, M.K., O'Brien, T.K., and Minguet, P.J., "Testing and Analysis of Composite Skin/Stringer Debonding Under Multi-Axial Loading," *Journal of Composite Materials*, Vol.34, No.15, 2000, pp.1264-1300.
5. Childress, J.J., and Freitas, G., "Z-direction Pinning of Composite Laminates for Increased Survivability," *Proceedings of the AIAA Aerospace Design Conference*, Irvine, California, USA, February 1992, Paper 92-1099.
6. Freitas, G., Magee, C., Dardsinski, P., and Fusco, T., "Fiber Insertion process for Improved Damage Tolerance in Aircraft Laminates," *Journal of Advanced Materials*, Vol. 24, July,1994, pp. 36-43.
7. B. Blaiszik, S.R. White, N.R. Sottos, "Nanocapsules for self-healing materials," *Composite Science and Technology*, 68:978-986 (2008).
8. K.S. Toohey, N.R. Sottos, J.A. Lewis, J.S. Moore, S.R. White, "Self-healing materials with microvascular networks," *Nature Materials*, 6:581-585 (2007).